JACS
JOURNAL OF THE AMERICAN CHEMICAL SOCIETY
Article
pubs.acs.org/JACS

Between Superexchange and Hopping: An Intermediate Charge-Transfer Mechanism in Poly(A)-Poly(T) DNA Hairpins

Nicolas Renaud,* Yuri A. Berlin, Frederick D. Lewis, and Mark A. Ratner

Department of Chemistry, Northwestern University, 2145 Sheridan Road, Evanston, Illinois 60208-3113, United States

Supporting Information

ABSTRACT: We developed a model for hole migration along relatively short DNA hairpins with fewer that seven adenine (A):thymine (T) base pairs. The model was used to simulate hole migration along poly(A)-poly(T) sequences with a particular emphasis on the impact of partial hole localization on the different rate processes. The simulations, performed within the framework of the stochastic surrogate Hamiltonian approach, give values for the arrival rate in good agreement with experimental data. Theoretical results obtained for hairpins with fewer than three A:T base pairs suggest that hole transfer along short hairpins occurs via superexchange. This mechanism is characterized by the exponential distance dependence of the arrival rate on the donor/acceptor distance, $k_a \simeq e^{-\beta R}$, with $\beta = 0.9$ Å^{-1}. For longer systems, up to six A:T pairs, the distance dependence follows a power law $k_a \simeq R^{-\eta}$ with $\eta = 2$. Despite this seemingly clear signature of unbiased hopping, our simulations show the complete delocalization of the hole density along the entire hairpin. According to our analysis, the hole transfer along relatively long sequences may proceed through a mechanism which is distinct from both coherent single-step superexchange and incoherent multistep hopping. The criterion for the validity of this mechanism intermediate between superexchange and hopping is proposed. The impact of partial localization on the rate of hole transfer between neighboring A bases was also investigated.

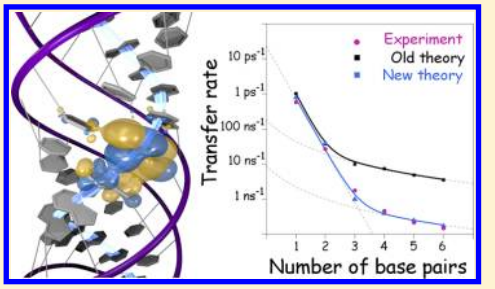

INTRODUCTION

The mechanism and dynamics of charge transfer in DNA continue to attract a lot of interest[1−4] due to its relevance to oxidative damage[5,6] and its potential application in molecular electronics[7,8] and biosensing techniques.[9,10] With a few exceptions,[11−15] most studies have focused on the migration of positive charges (holes). The propagation of these charge carriers was recently probed using time-resolved pump−probe spectroscopy. For this purpose, the hairpins are capped with a hole donor (S_a) at one end and a hole acceptor (S_b) at the other. Stilbenecarboxamide/stilbenediether[16,17] and naphthalimide/phenothiazine[18,19] are the most commonly used chromophores due to their favorable electronic structure. A detailed description of the femtosecond broadband pump−probe spectroscopy setup used by Lewis et al. can be found elsewhere.[20] Photoexcitation of the hole donor by a pump wavelength (333/355 nm) induces a one electron transition to the LUMO, thus generating a hole on the HOMO. This hole can propagate along the hairpin and eventually reach the hole acceptor where it can be detected using a femtosecond white-light continuum (300−755 nm).

The sequence of base pairs inside the DNA hairpin affects significantly the hole transfer from S_a to S_b.[18,21−24] Homogeneous sequences containing only guanine-cytosine (G:C) base pairs exhibit relatively high hole mobility[25−29] due to larger electronic coupling of the guanines[30] and the lower ionization potential of these bases as compared to A bases.[30−33] By contrast, sequences containing only adenine-thymine (A:T) base pairs show a smaller hole mobility[34] mainly mediated by the adenine tract.[35] Insertion of a single[28,36] or several consecutive G:C[27] base pairs in a poly(A)-poly(T) hairpin increases significantly the mobility of holes. This effect depends on the position of the G:C base pairs in the sequence, and the most significant changes in transport properties have been observed when the G:C base pair is located at the end of the sequence. It should also be noted that the introduction of modified base pairs, such as 7-deazaadenines[18,37] or locked nucleic acids,[38] has been shown to dramatically change the charge-transfer properties of short hairpins.

Considerable progress in time-resolved spectroscopic techniques makes it possible to characterize the overall process of hole transfer across DNA hairpins in sufficient detail. However the mechanism by which the hole propagates along the hairpins is still under discussion. Superexchange is thought to be responsible for charge transfer along very short hairpins with 1−3 base pairs. When charge transfer is dominated by superexchange, the hole directly tunnels from the donor to the acceptor using the base pairs as virtual states.[39−42] As a consequence the charge transfer rate decreases with the distance, R, following an exponential law:[3,22,34,43]

$$k_a(R) = k_0 e^{-\beta R} \quad (1)$$

with $\beta \sim 1.0$ Å^{-1} is the falloff parameter[44,45] and k_0 is a pre-exponential scaling factor. For longer hairpins however a transition from superexchange to incoherent hopping is

Received: December 3, 2012

   dx.doi.org/10.1021/ja3113998 | J. Am. Chem. Soc. XXXX, XXX, XXX−XXX

assumed to occur, and the latter mechanism becomes dominant.[22,46−49] Incoherent hopping along the stack containing A:T or G:C base pair separated by an average distance R_0 leads to a weak distance dependence of $k_a(R)$.[22,25,50] In this case the arrival rate can be described by a power law[39,49,51−54]

$$k_a(R) = k_0(R/R_0)^{-\eta} \quad (2)$$

or by a rational function[55,56]

$$k_a(R) = \frac{a}{1 + bR} \quad (3)$$

where the coefficients a and b depend on the rates of the elementary steps involved in the charge-transfer process. It is worth mentioning that in the case of incoherent hopping in DNA, the hole is often assumed to be confined to a single base pair due to the important static and dynamic disorder in the system. The hole then propagates between neighboring sites by a series of hops. The nature of these hops remains the subject of vivid debates mainly because of the poor understanding of the charge localization/delocalization phenomenon in DNA.

If the hole density is extended over several base pairs as a result of polaron formation,[57−60] hole propagation can be considered as sequential phonon-assisted polaron hopping[61] or in terms of transient delocalized domains.[62] Such delocalization of the hole density is to be expected due to the interactions between neighboring base pairs. However polarization effects of the surroundings,[63] internal reorganization of the base pairs,[64] and dephasing caused by the geometrical fluctuations of the DNA hairpins are thought to significantly reduce this charge delocalization. As a consequence, the idea of charge delocalization in DNA hairpins is often rejected or at least limited to a few pairs only.[65]

Many time-dependent quantum mechanical studies have been performed to understand the crossover between tunneling and hopping regime and its relation to the charge localization/delocalization phenomenon.[23,24,40,42,65,66] In these studies, the interactions of the hole with its environment were modeled using either the time-dependent self-consistent field approach,[23,40,66] the Su−Schrieffer−Heeger model,[65] or uncorrelated fluctuations.[24,42] To simplify the analysis, it was assumed that with the exception of multiple guanine units, the charge relaxation inside each individual base is slower that the rate of transition to the neighboring base, so that for each base pair only a single quantum state is involved in the migration process.[40,67−69] Molecular Dynamics (MD) simulations coupled with standard electronic structure calculations were employed to compute the energy of these states as well as the electronic coupling between pairs.[42,70] These calculations have revealed large temporal fluctuations of these quantities induced by geometrical deformations of the hairpins.[42,66,71,72] Note that this dynamical disorder is beneficial for hole transfer since it helps a charge carrier to overcome the barrier formed by the electrostatic interactions between the propagating hole and the anion of the hole donor.[38,42,66,73] Although in the case of short hairpins containing 1−2 base pairs, calculations based on the approach discussed above give results consistent with experimental findings, for longer hairpins only qualitative agreement between theory and experiment has been attained. The poor quantitative agreement in the latter case was attributed to the fact that the theoretical models proposed so far ignore relaxation of the system geometry[42,64] and the partial localization of the hole density in DNA sequences.[74] To verify the validity of this explanation, one should take into account decoherence and relaxation in the model used to simulate the charge motion along DNA hairpins.

Several theories have been developed to include decoherence and relaxation while keeping a correct description of the coherent phenomenon.[75] The usual Redfield and Lindblad approaches are commonly used for this purpose.[76,77] Both of these historic approaches are nowadays often replaced by analytical[78] or numerical[79,80] non-Markovian approaches that avoid the perturbative treatment of the system/bath interactions. Here the propagation of the hole density is simulated using the stochastic surrogate Hamiltonian (SSH) approach.[81−83] In this framework, a few bath modes are explicitly treated in the total Hamiltonian.[84,85] The Liouville equation is then solved for the extended system, modeling the hairpin together with these few bath modes. Quantum jumps are performed in the bath manifold to limit the computational cost of the SSH approach.[83] Since quantum jumps are stochastic events and the bath spectral density is sampled randomly, the SSH approach has clear statistical features. For this reason the Liouville equation must be solved a few hundred times to converge to the final dynamics. This allows the accurate simulation of the dynamics of an open quantum systems in the nanosecond time range and at affordable computational cost.[83,86]

The computational studies discussed in this paper deal with the coherent motion of the hole along poly(A)-poly(T) sequences containing 1−6 A:T base pairs (referred to 1, 2, ..., 6, respectively) accompanied by the incoherent processes caused by the interaction of the propagating charge with the molecular vibration modes of the system. The coherent propagation of the hole is described by a tight-binding Hamiltonian (see, e.g., ref 40), while the environment of the propagating charge is assumed to include both classical and quantum modes responsible for the incoherent dynamics. The classical modes correspond to large deformations of the hairpin associated with the tilt, roll motion of base pairs, and the dynamics of other degrees of freedom that define π-stack geometry. Such modes serve as the origin of dynamic disorder that randomly modifies the parameters of the electronic Hamiltonian. This dynamical disorder dephases the coherent propagation, but does not cause energy relaxation. The description of the latter process requires the consideration of the quantum modes related to the intramolecular vibrations of the A:T pairs in the DNA hairpins. The hole−phonon interactions are modeled within the SSH approach and are the source of energy dissipation in our calculations. Due to the presence of localizing states in our model, the hole density is partially localized during the coherent propagation along the stack of A:T pairs. This partial localization of the moving hole is distinct from the temporary trapping of charge carriers in the course of hopping. The traditional hopping transport mechanism suggests the localization of all hole density (rather than its part) on a single A base.

Proton transfer necessary to the formation of the charged radical observed experimentally is not included in our model. Charge and proton transfers are assumed to occur sequentially, and the possibility of proton-couple-electron transfer[87,88] is not explored in this article. It should also be mentioned that our model does not take into account the reorganization of the solvent around the hairpin during the hole propagation and the charge localization effects induced by the polar surrounding.[63] Consequently our analysis is only valid for relatively short hairpins for which hole propagation from S_a to S_b is faster than

dx.doi.org/10.1021/ja3113998 | J. Am. Chem. Soc. XXXX, XXX, XXX−XXX

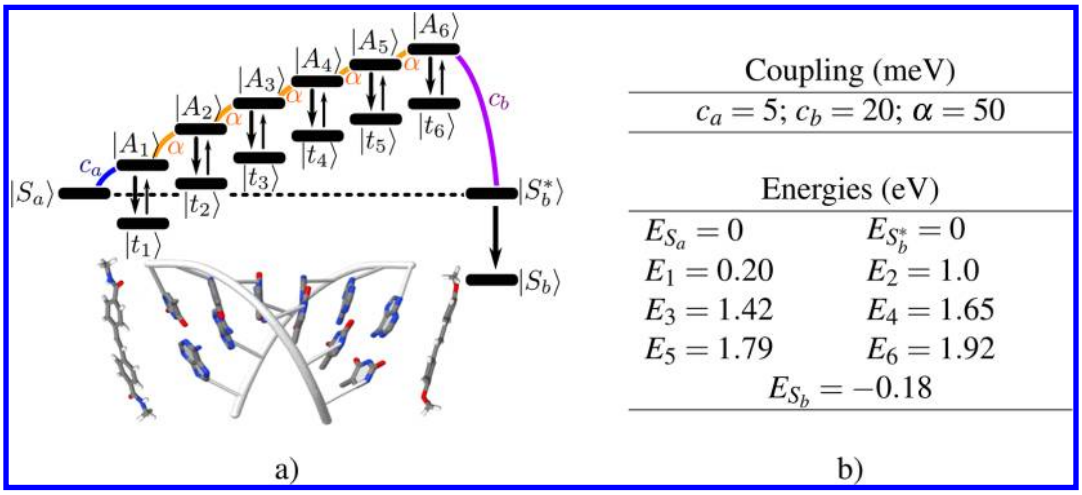

Figure 1. Schematic representation of the model used to study the hole propagation across the hairpin **6** (a) and parameters of the model (b). Starting from the hole donor $|S_a\rangle$ the hole propagates on the states $|A_n\rangle$. The hole density can be partially localized on the $|t_n\rangle$ states and possbily thermally activated later on. The hole density can eventually reach the hole acceptor excited state $|S_b^*\rangle$ before the final localization of the hole on the ground state of acceptor $|S_b\rangle$ occurs.

the time needed for the solvent to reorganize. For longer hairpins, such localization effects are not negligible and require special consideration.[57]

MODEL

Hamiltonian. The model used to study the propagation of the photogenerated hole along a short poly(A)-poly(T) hairpin with N nucleobases is schematically shown in Figure 1. In this model, the hole donor is represented by a single quantum state $|S_a\rangle$. The n-th base pair (n = 1, 2, ..., N) in the sequence is modeled by a conducting state $|A_n\rangle$ and a hole localized state $|t_n\rangle$. Similarly, two states are used to characterize the hole acceptor. These include an excited state of the acceptor cation $|S_b^*\rangle$ and the cation ground state $|S_b\rangle$. Within the tight-binding approximation, the model Hamiltonian can be written as

$$\begin{aligned}\mathcal{H}_S = {} & E_{S_a}|S_a\rangle\langle S_a| + \sum_{i=1}^{N} E_i|A_i\rangle\langle A_i| + E_{S_b^*}|S_b^*\rangle\langle S_b^*| + c_a|S_a\rangle\langle A_1| \\ & + \alpha \sum_{i=1}^{N-1} |A_i\rangle\langle A_{(i+1)}| + c_b|A_N\rangle\langle S_b^*| \\ & + h.c. + \sum_{i=1}^{N} (E_i - E_{\mathrm{loc}})|t_i\rangle\langle t_i| + E_{S_b}|S_b\rangle\langle S_b| \end{aligned} \quad (4)$$

In eq 4 $|S_a\rangle$ is the initial state of the hole density with an energy E_{S_a}. All the other energies involved in the model are counted from E_{S_a}. Therefore we can set this reference energy equal to zero. The measure of the electronic coupling between various sites in our model is the transfer integrals c_a, c_b, and α. The first quantity c_a describes the coupling between the donor and the first hairpin site. The coupling between the last A:T base pair and the hole acceptor is given by the second transfer integral, c_b, while α denotes a coupling between neighboring A:T bases in the poly(A)-poly(T) sequence. The state $|A_1\rangle$ corresponds to a the situation where a hole is located on the first A base, thus generating an anion on the donor site. This ion pair is symbolized as S_a^-/A_1^+. The hole propagates along the hairpin via the states $|A_n\rangle$ forming the intermediate ion pairs S_a^-/A_n^+ and eventually reaches the excited state of the acceptor, $|S_b^*\rangle$, that can subsequently undergo relaxation to the ground state $|S_b\rangle$. Shallow localizing states, $|t_n\rangle$, are also incorporated in our model. Their energies are smaller than the energy of the $|A_n\rangle$ state by the value of the localization energy, E_{loc}, which is the only variable parameter in our simulations. Other parameters of the model were either estimated or taken from the literature as explained in the next section.

Parameters. Following recent calculations,[42] the values of the energies E_n for a particular A site can be estimated using the Weller-like relation:

$$E_n = \mathrm{IP_A} - E_{h\nu} - \mathrm{EA}_{S_a} + E_c(S_a^-/A_n^+) - \Delta E_{\mathrm{solv}} \quad (5)$$

Here, $\mathrm{IP_A}$ = 7.35 eV is the ionization potential of the adenine,[30,33] EA_{S_a} = 1.08 eV is the electron affinity of the hole donor,[42] $E_{h\nu}$ = 3.35 eV its excitation energy,[34] $E_c(S_a^-/A_n^+)$ is the electrostatic interactions between the negative charge located on S_a and the propagating hole, and ΔE_{solv} = 0.2 eV is the solvation energy.[42] With $E_c(S_a^-/A_n^+)$ calculated within a point charge approximation and the above-mentioned values of the other parameters, eq 5 yields values of the on-site energies ranging from E_1 = 0.20 eV up to E_6 = 1.92 eV.[42]

To take into account for the possibility of single-step superexchange between S_a and S_b, the energy of the acceptor excited state, $|S_b^*\rangle$, is chosen to be in resonance with the hole donor (i.e., $\mathrm{E}_{S_b^*}$ = 0.0 eV) . The energy of the cationic ground state $|S_b\rangle$ is determined following eq 5 using the ionization potential of the hole acceptor. Gas-phase calculation gives the ionization potential of the hole acceptor: IP_{S_b} = 6.35 eV. However this value is expected to be reduced by ~0.7 eV in solution.[30] The site energy of $|S_b\rangle$ should in principle depend on the length of the hairpin because of the Coulombic potential term in eq 5. However, for our calculations not to be dominated by the energetic of the hole acceptor, we fix the energy of $|S_b\rangle$ equal to the value E_{S_b} = −0.18 eV obtained by averaging over the lengths of various poly(A)-poly(T) hairpins.

Due to the thermal deformation of the DNA strands, the site energies are subjected to random Gaussian fluctuations with a standard deviation of 0.15 eV and the average time of τ_E = 0.1 ps.[42] On the basis of earlier computational results[42,70] a weak average coupling of c_a = 5 meV is assumed between the hole donor and the first base pair. Larger values of the transfer

dx.doi.org/10.1021/ja3113998 | J. Am. Chem. Soc. XXXX, XXX, XXX−XXX

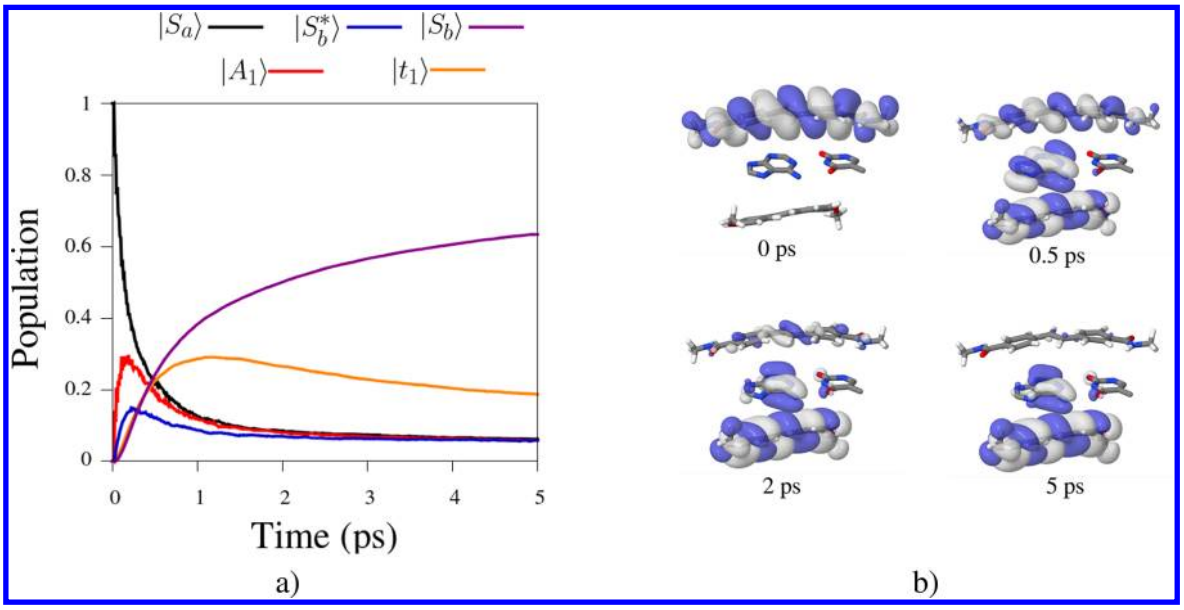

Figure 2. Hole propagation along hairpin **1**. Temporal evolution of the hole density over the period of 5 ps. The temporal evolution of hole population on the donor site, on the excited and ground states of the acceptor as well as on the adenine sites are shown by different colors. (b) Snapshots of the hole density at different times.

integrals α = 50 meV and c_b = 20 meV characterize the electronic coupling between neighboring adenines and between the last A:T base pair and the hole acceptor, respectively. These couplings are also subjected to strong fluctuations described by random Gaussian distributions with a standard deviation of 50 meV and the average time of τ_c = 0.5 ps.[42] These random fluctuations of the site energies and transfer integrals model uncorrelated classical modes which dephase the coherent charge propagation without inducing energy relaxation.

The impact of partial localization on the hole propagation strongly depends on the value of the localization energy, E_{loc}. Certainly, this energy depends on the mechanism of localization considered. The geometry relaxation of a given base pair upon charging is one of the principal localization process. The corresponding localization energy can be estimated by comparing the vertical and adiabatic ionization potential of the adenine. This leads to E_{loc} values ranging from 0.18 to 0.36 eV.[64] Other mechanisms responsible of partial localization includes the formation of a delocalized triplet with a typical localization energy of a few meV.[74] Therefore several values of the localization energy ranging from 50 to 250 meV were employed in our calculations.

HOLE–PHONON INTERACTION

The propagation of the hole across the poly(A)-poly(T) hairpin is computed using the Hamiltonian given by eq 4 and the SSH approach to take into account relaxation and decoherence. Similar to the methods developed to simulate the evolution of open quantum systems,[75] the SSH approach considers the Hamiltonian $\mathcal{H}$ as the sum of three terms:

$$\mathcal{H} = \mathcal{H}_S + \mathcal{H}_B + \mathcal{H}_{SB} \tag{6}$$

where $\mathcal{H}_S$ is the Hamiltonian of the system described by eq 4, $\mathcal{H}_B$ stands for the Hamiltonian of the bath, and $\mathcal{H}_{SB}$ denotes the interaction between the system and the bath. The bath is modeled by an ensemble of M noninteracting two level systems, or quantum modes. The corresponding bath Hamiltonian is defined by

$$\mathcal{H}_B = \sum_{i=1}^{M} \omega_i \boldsymbol{\sigma}_i^\dagger \boldsymbol{\sigma}_i \tag{7}$$

where ω_i is the energy of the i-th mode and $\boldsymbol{\sigma}_i^\dagger$ ($\boldsymbol{\sigma}_i$) the creation (annihilation) operator. This fully quantum treatment of the bath modes allows for a rather accurate simulation of system/bath entanglement and energy relaxation.[81]

The Hamiltonian describing the interactions between the system and the environment can be written as

$$\mathcal{H}_{SB} = \mathcal{R}_S \otimes \sum_{i=1}^{M} \frac{\mathcal{J}(\omega_i)}{\sqrt{M}} (\boldsymbol{\sigma}_i^\dagger + \boldsymbol{\sigma}_i) \tag{8}$$

where $\mathcal{R}_S$ is the relaxation pathway matrix,[83] $\mathcal{J}(\omega_i)$ the spectral density of the bath, evaluated at the bath-mode energy ω_i, and M the number of bath modes explicitly accounted for in the Hamiltonian. According to our model (see Figure 1), partial localization of positive charge can be viewed as the transition from the $|A_i\rangle$ to the $|t_i\rangle$ state as well as the transition from $|S_b^*\rangle$ to $|S_b\rangle$. Then the relaxation matrix reads:

$$\mathcal{R}_S = (|S_b^*\rangle\langle S_b| + \sum_{i=1}^{N} |A_i\rangle\langle t_i|) + h.c. \tag{9}$$

The Hamiltonian $\mathcal{H}_{SB}$ introduces indirect coupling via the bath modes between the $|A_i\rangle$ and $|t_i\rangle$ states as well as between excited state of the hole acceptor $|S_b^*\rangle$ and its ground state $|S_b\rangle$. Consequently localization occurs only on a given molecule, either a base pair or the hole acceptor. Hence this process is assisted by the intramolecular vibration modes of the molecules. To model the phonon bath formed by these modes, the bath spectral density is defined as a super-ohmic distribution:[89,90]

$$\mathcal{J}(\omega) = \lambda(\omega/\omega_c)^2 e^{-(\omega/\omega_c)^2} \tag{10}$$

with the cutoff energy, ω_c, set to ω_c = 0.15 eV to in order to fit eq 10 to the intramolecular vibration spectrum of the adenine molecules.[91] The inner-shell reorganization energy, λ, quantifies

dx.doi.org/10.1021/ja3113998 | J. Am. Chem. Soc. XXXX, XXX, XXX–XXX

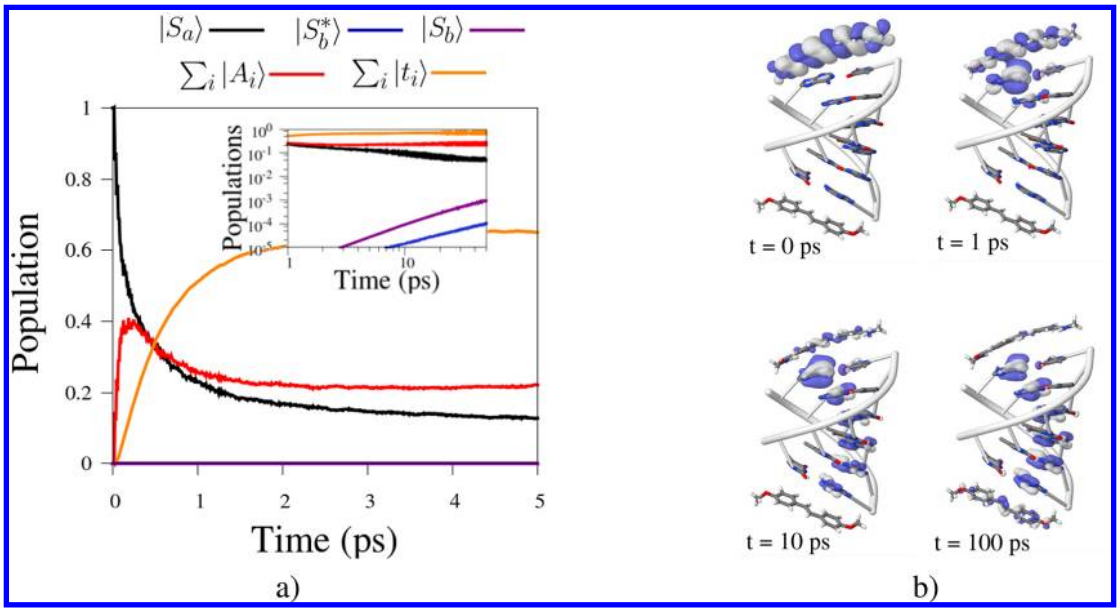

Figure 3. Hole propagation along hairpin **6**. (a) Temporal evolution of the hole density over the period of 10 ps. The temporal evolution of hole population on the donor site, on the excited and ground states of the acceptor as well as on the adenine sites are shown by different colors. (b) Snapshots of the hole density at different times which show the degree of hole delocalization at different times on the ps scale.

interactions between the hole and the molecular vibrations modes. For A:T base pairs, the hole−phonon coupling ranges from 1 to 250 meV depending on the vibrational mode considered.[92] The estimations of the internal reorganization energy of the base pairs provide values close to 150 meV.[64] To describe these various hole−phonon interactions with a single parameter, we set the reorganization energy equal to λ = 100 meV. However variations of λ by a factor of 2 do not change significantly our results. Using the spectral density defined by eq 10 leads to strong hole−phonon interactions for the breathing modes of the molecules around 0.15 eV and weaker interactions for the low- and high-frequency modes.[92]

Once the three components of the total Hamiltonian are properly defined, the propagation of the density matrix, $\rho(t)$, is computed solving the Liouville equation:

$$\frac{d\rho(t)}{dt} = -\frac{i}{\hbar}[\mathcal{H}, \rho(t)] \tag{11}$$

To simulate the evolution of the system for few picoseconds at an affordable computational cost, only a few bath modes are explicitly treated in eq 7. In addition quantum jumps are introduced in the bath manifold.[81,82] Each of these jumps reset the reduced density matrix of one given mode to its thermal state, removing a small amount of energy from the extended system.[83] Due to the random sampling of the bath spectral density and the stochastic quantum jumps, the SSH approach is a statistical treatment of the dynamics of an open quantum system. Consequently the dynamics was computed 500 times to converge toward the final temporal evolution. The initial state of the dynamics is defined as

$$\rho(0) = \rho_S(0) \otimes \rho_B(T) \tag{12}$$

where $\rho_S(0) = |S_a\rangle\langle S_a|$ and $\rho_B(T)$ is a thermal state of the bath. This nonentangled initial state supposes that the photoexcitation of the system destroys pre-existing system/bath entanglement. Once the dynamics is solved, the temporal evolution of the hole density on the DNA hairpin is extracted from the total density matrix by tracing out the bath modes:

$$\rho_S(t) = Tr_B[\rho(t)] \tag{13}$$

A more detailed description of the implementation of the SSH approach as well as a brief description of the decoherence and energy relaxation mechanisms induced by the system/bath interactions can be found in Supporting Information (SI).

RESULTS AND DISCUSSIONS

Hole Dynamics. Figure 2a shows the temporal evolution of the hole population along hairpin **1** at room temperature and in the case of E_{loc} = 150 meV. As can be seen from this figure, a fast charge transfer occurs from the hole donor, $|S_a\rangle$ to the excited state of the acceptor $|S_b^*\rangle$. This fast transfer is due to a superexchange between these resonant states via the A base acting as a small energy barrier. The data plotted in this figure show that after 0.25 ps, 17% of the hole density has already crossed this ultrashort DNA strand and has reached the excited state of the hole acceptor. When reaching this excited state, the hole undergoes an irreversible transition to the ground state $|S_b\rangle$. This localization process leads to a fast increase of the population of $|S_b\rangle$ that accounts for more than 60% of the hole density after 5 ps. Due to the partial localization on the A base, the population of the localized state, $|t_1\rangle$, slowly increases with time and accumulates up to 25% of the hole density after 1 ps. For longer times, the hole density is able to escape this shallow trap by thermal activation. The latter process is responsible for the slow decrease of the population of $|t_1\rangle$ evident from Figure 2a.

Snapshots of the hole density are represented in Figure 2b. The subpicosecond transfer from the donor to the acceptor due to single-step superexchange is clearly seen. The hole density turns out to be completely delocalized over the entire system (i.e., the hole donor, acceptor, and the AT base pair) after 0.5 ps, i.e., before irreversible localization of positive charge on the acceptor ground state.

Figure 3a shows the propagation at the room temperature of a photogenerated hole along hairpin **6** with a localization energy of E_{loc} = 150 meV. Snapshots of the hole density are

dx.doi.org/10.1021/ja3113998 | J. Am. Chem. Soc. XXXX, XXX, XXX−XXX

represented in Figure 3b. After the photoexcitation, the hole is rapidly injected from the $|S_a\rangle$ to $|A_1\rangle$ where 40% of the population is localized after only 0.1 ps. For this relatively long hairpin, superexchange between the hole donor and acceptor does not make a major contribution to the mechanism of hole transfer. Consequently, the population of $|S_b\rangle$ does not rapidly increase as observed for hairpin **1**. This can be expected since the hole formed in hairpin **6** has to overcome a large Coulomb potential to reach the hole acceptor. This latter process becomes possible due to the dynamic disorder that creates random resonances between the $|A_i\rangle$ states, thus facilitating the charge transport across the system.[42] This fluctuation-gated hole transfer is much slower than the superexchange mediated transfer along hairpin **1**, and the population of the $|S_b\rangle$ states increases only by fraction of a percent after 50 ps. Hence the hole density is mainly localized on the A:T base pairs. Furthermore our results show that 60% of the hole density is partially localized on the $|t_i\rangle$ states after 5 ps. The hole dynamics depicted in Figure 3 cannot be associated either with superexchange or with the common hopping mechanism described in the literature. The charge propagation along this hairpin occurs via intermediate charge-transfer mechanism, which is discussed and compared with other relevant theoretical findings in the Charge-Transfer Mechanism section. This intermediate charge-transfer mechanism is discussed and compared with other models in this section of the manuscript. As seen in Figure 3, a striking characteristic of this intermediate mechanism is the delocalization of the charge density along the entire hairpin. This delocalization, however, does not contradict the oxidation of the base pairs observed in steady-state experiments.[21] The latter is obviously distinct from time-resolved measurements that are the focus of this study.

Arrival Rate of Holes on the Acceptor Site. The hole arrival rate at the hole acceptor, k_a, and the charge separation quantum yield, Φ_{CS}, are the main observables used to quantify hole transfer along stacked base pairs. Experimentally, these two quantities are deduced from the time-dependent band intensity ratio of the anion S_a^- and the cation S_b^+.[27] Using our simulations k_a and Φ_{CS} can be evaluated by fitting the calculated population of $|S_b\rangle$ with the rising exponential function:

$$Tr[|S_b\rangle\langle S_b|\rho_S(t)] = \Phi_{CS}(1 - \exp(-k_a t)) \quad (14)$$

Fitting the population of the hole acceptor located at the end of hairpin **1** with eq 14 leads to $k_a = 0.65$ ps^{-1} and $\Phi_{CS} = 0.87$. This very fast transfer rate and high quantum yield are in good agreement with the recent experimental data which give $k_a = 0.58$ ps^{-1} and $\Phi_{CS} = 1$.[34] For hairpin **6**, the similar fitting gives a much smaller arrival rate, $k_a = 0.17$ ns^{-1} and very low quantum yield $\Phi_{CS} = 0.09$, which are again in good agreement with experimental data (see Table 1). As it can be seen from this table, the values of the arrival rate obtained with our approach are in reasonable agreement with experiments for all the hairpins studied. Although our predictions for the quantum yield agrees with the experimental results for hairpin **1** and **6**, they underestimate Φ_{CS} for all the other hairpins. It should be mentioned however that the distance dependence of the quantum yield obtained in the framework of our model was found to be in close agreement with earlier experiments on the so-called damage ratio.[50] The latter quantity which is proportional to Φ_{CS}, decreases rapidly as the number of A:T base pairs in the hairpins increases from 1 to 3 but does not show any significant changes for longer sequences.

Table 1. Experimental and Theoretical Values of the Arrival Rate and Charge Separation Quantum Yield for Hairpins 1−6

	theory[a]		experiment[b,c]	
seq.	Φ_{CS}	k_a 10^{10} s^{-1}	Φ_{CS}	k_a 10^{10} s^{-1}
1	0.87	65.39	1.00	58.00
2	0.34	4.47	0.80	2.50
3	0.13	0.13	0.52	0.40
4	0.09	0.05	0.23	0.10
5	0.09	0.03	0.10	0.02
6	0.09	0.02	0.09	0.01

[a]Theoretical values were obtained assuming that E_{loc} = 150 meV. [b]Experimental values for Φ_{CS} were taken from ref 36. [c]Experimental values for k_a were taken from ref 35.

Many investigations suggest that the dependence of the arrival rate on the number, N, of the A:T base pairs in the sequence (and hence on the distance between hole and acceptor R) might be important for the identification of the mechanism governing hole transfer, see, e.g., refs 4, 39, 51, 52, and 61. The distance dependence of the arrival rate obtained for different values of the localization energy and for the case where partial localization is ignored is shown in Figure 4. In this

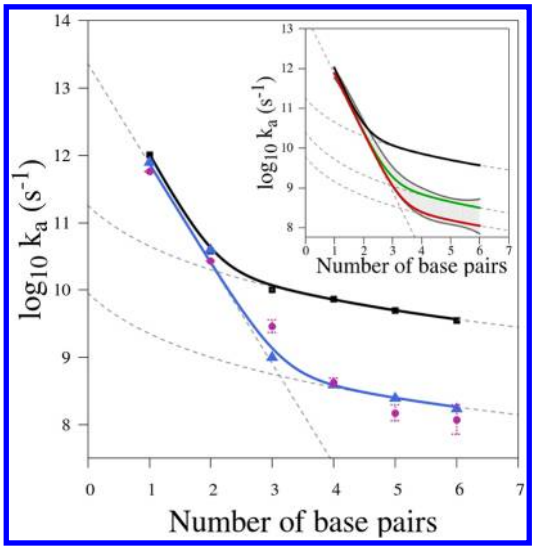

Figure 4. Hole arrival rate on the acceptor site, k_a, obtained from our simulations as a function of the number of A:T base pairs in hairpins with the poly(A)-poly(T) sequence. Calculations were performed without temporal localization (black curve), with the localization energy equal to 150 meV (blue curve), 50 meV (green curve in the insert) and 250 meV (red curve in the insert). Computational results are shown by triangles and squares. Solid lines correspond to the approximation of these results by eq 15. Dashed lines represent two terms of eq 15. Purple dots are the experimental data taken from ref 35. The shaded area in the insert includes the experimental values of k_a reported in different publications.[27,28,34−36]

figure R is expressed in terms of the number of the A:T base pairs between these two sites. The values of k_a as a function of R deduced from our simulations can be approximated by the function:

$$k_a(R) = \kappa_1 e^{-\beta R} + \kappa_2 (R/R_0)^{-\eta} \quad (15)$$

where κ_1 and κ_2 are scaling factors and $R_0 = 3.40$ Å is the distance between two neighboring A:T base pairs. Note that the

dx.doi.org/10.1021/ja3113998 | J. Am. Chem. Soc. XXXX, XXX, XXX−XXX

incorporation of partial localization in the model of hole transfer improves considerably the agreement between theoretical and experimental results as follows from comparison of black and blue solid lines with purple dots in Figure 4.

Fitting eq 15 to the results of our simulations, we found that $\kappa_1 = 0.7$ fs^{-1} and $\beta = 0.9$ Å^{-1} with both parameters being independent of E_{loc}. The independence of κ_1 and β to the localization energy confirms that superexchange is responsible for the hole transfer along short hairpins. During superexchange, the hole density is directly transferred from the donor to the acceptor without visiting A:T sites that are used as virtual states. Therefore the presence of trapping states along the hairpin and the value of the localization energy are irrelevant to this regime. The value of β obtained by this fit is consistent with experimental data that gives $\beta = 0.5-1.0$ Å^{-1}.[93−95] This value is extremely sensitive to the difference between the energy of the hole donor and the energy of the base pair. Consequently changing the nature of the photosensitizers or the base pair should significantly modify the value of the falloff parameter.[95]

The exponent of the power law term in eq 15 deduced from out results for long-range charge transfer (hairpins **3**−**6**) was found to be equal to $\eta = 2$, i.e., slightly larger that the experimental value $\eta = 1.5-1.7$.[51,96] In addition, it is evident that variations of E_{loc} do not affect the value of the exponent η but reduce the scaling factor κ_2. According to the data presented in Figure 4, the value of this parameter decreases from 180 ns^{-1} in the absence of partial localization to 25 ns^{-1} for $E_{loc} = 50$ meV and becomes equal to 7 ns^{-1} for $E_{loc} = 250$ meV.

The formal similarity of eq 15 and the expression for k_a derived earlier[67] to take into account the competition of hole tunneling and thermal activation hopping implies that the distance dependence of the arrival rate alone is insufficient for making convincing conclusions about the mechanism of hole migration in DNA hairpins. Indeed, eq 15 describes equally well two distinct processes of charge transfer, namely tunneling of holes competing with their hopping and the fluctuation-gated motion of positive charges accompanied by partial localization of charge density.

Rate of Hole Injection. Another important elementary process involved in the mechanistic picture of hole transfer is the injection rate of a positive charge onto the stack of base pairs. Experimentally, the hole dynamics for stilbenediamide/stilbenediether-capped hairpins with 1−7 intervening A:T base pairs was deduced from the analysis of the fluorescence and transient absorption data.[28] In particular, the observed picosecond and nanosecond fluorescent decays were assigned to fast and slow hole injection processes.

Our model enables us to evaluate the characteristic times of these decays and, hence, the fast and slow injection rates, k_i^f and k_i^s, using the time evolution of hole population calculated for the $|S_a\rangle$ state. As seen in Figures 2 and 3, the hole population on $|S_a\rangle$ decreases biexponentially in time so that the following relation is valid:

$$Tr[|S_a\rangle\langle S_a|\rho_S(t)] = \sum_{n=f,s} \Phi_i^n e^{-k_i^n t} \quad (16)$$

where Φ_i^f and Φ_i^s are the quantum yield for the fast and slow processes, respectively. The values of the injection rates and quantum yields were deduced by fitting the temporal evolution of $|S_a\rangle$ with eq 16 and are presented in Table 2 along with available experimental values.[34] As can be seen from this table,

Table 2. Rate (k_i^f, k_i^s) and Quantum Yields (Φ_i^f, Φ_i^s) for Fast and Slow Injection into Poly(A)-Poly(T) Hairpins

	theory[a]				experiment[b]			
seq.	k_i^f (ps^{-1})	Φ_i^f	k_i^s (ps^{-1})	Φ_i^s	k_i^f (ns^{-1})	Φ_i^f	k_i^s (ns^{-1})	Φ_i^s
1	4.44	84	0.57	9	–	–	–	–
3	3.29	78	0.17	12	15.15	76	2.70	20
6	3.32	80	0.12	14	10.52	71	1.12	19

[a]Theoretical values are obtained for a localization energy of 150 meV. [b]Experimental data were taken from ref 34.

the injection quantum yields Φ_i^f and Φ_i^s obtained with our approach are in good agreement with the experimental data; however, our model overestimates the hole injection rates by 2 orders of magnitude as compared to experimental values reported in ref 34. This may be a consequence of the limited time resolution of the fluorescence decay measurements. Subsequent reanalysis of the femtosecond transient absorption data for S_a-linked hairpins suggests that hole injection occurs within the first few picoseconds following laser excitation.[28] It is also possible that excitation directly populates a charge-transfer state, thereby bypassing the hole injection process and leading directly to the hole populations obtained by our model after ∼1 ps (see Figures 2 and 3).

Rate of Hole Transfer between Neighboring Base Pairs. In addition to the rates of hole injection and arrival on the acceptor site, the obtained numerical results also allow estimations of the rate of positive charge transfer between neighboring A:T base pairs. It should be emphasized again that our simulations lead to a delocalization of the hole density along the hairpin. Therefore, the hole transfer between two adjacent base pairs considered in this section has nothing in common with hopping. The latter requires a complete localization of the hole density on a single site rather than the partial localization of this density. A scheme illustrating the method employed to evaluate the rate, $k_{n\to n+1}$, for hole transfer between the n-th and the $(n + 1)$-th base pairs is shown in Figure 5 using hairpin **3** as an example.

To compute the elementary transfer rate, $k_{n\to n+1}$, between the n-th and $(n +1)$-th A:T base pair, the hole population of these two sites is first fitted by an exponential function similar to eq 14. This fit provides the values of the rates k_n and k_{n+1} of the hole transfer from S_a to the n-th base pair and from S_a to the

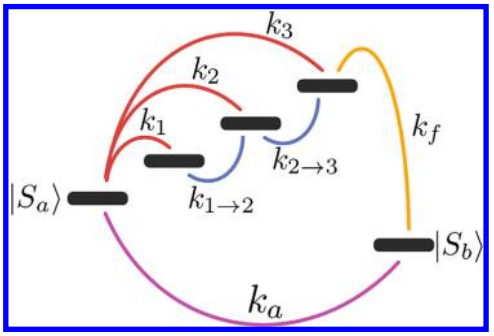

Figure 5. Schematic illustration of the method for evaluation the hole transfer rates between neighboring A:T base pairs in hairpin **3**. Rates, k_n, for hole transfer from the donor state $|S_a\rangle$ to the n-th A:T pair are obtained from our numerical calculations. The transfer rates $k_{n\to(n+1)}$ are deduced from the rates k_n and k_{n+1} via eq 17. Similarly the rate of hole transfer from the last A:T to the acceptor state $|S_b\rangle$ was estimated exploiting calculated values of k_3 and k_a.

dx.doi.org/10.1021/ja3113998 | J. Am. Chem. Soc. XXXX, XXX, XXX−XXX

$(n + 1)$-th base pair, respectively (see Figure 5). The characteristic time, τ_{n+1}, of charge transfer from the donor site to the $(n + 1)$-th base pair can be expressed as the sum of the time, τ_n, needed to transfer a positive charge from the donor to the n-th base pair and the time, $\tau_{n\rightarrow n+1}$, of hole transfer between the n-th and $(n + 1)$-th site. Since $k_{n\rightarrow n+1} = \tau^{-1}_{n\rightarrow n+1}$, the transfer rate between neighboring A:T base pairs can be expressed in terms of k_n and k_{n+1} as

$$k_{n\rightarrow n+1} = \frac{k_n \times k_{n+1}}{k_n - k_{n+1}} \quad (17)$$

The values of the hole transfer rate between neighboring base pairs calculated for hairpin **6** using eq 17 with different values of E_{loc} are summarized in Table 3. Numerical data obtained for the case where partial localization is ignored are also included in the table. Due to the gradual reduction of the energy gap between neighboring sites (see Figure 1), the values of $k_{n\rightarrow n+1}$ $(n = 1-5)$ are larger at the end of the hairpins (1.8–4.3 ps^{-1}) than at the beginning (0.18–0.36 ps^{-1}). Besides, the hole transfer between neighboring A:T pairs decreases significantly when partial localization is taken into account. Deeper traps make thermal repopulation of the $|A_i\rangle$ states more difficult thus reducing the interbase pair transfer rates (see SI for more details). Previous theoretical estimations of the transfer rate between the nearest neighbors in the base pair stack lead to a value of 0.3 ps^{-1}[97] and 1.2 ns^{-1},[98] while the values deduced from some time-resolved measurement equals 20 ns^{-1}.[96] This experimental estimate is at least 2 orders of magnitude lower than our numerical results (see Table 3). Note, however, that analysis of experiment in ref 96 and the calculations performed in the present work refer to diametrically opposed situation. While the experimental estimate was made assuming that the transfer from the last base pair to the hole acceptor k_f is much faster than the interbase pair transfer rate $k_{n\rightarrow n+1}$,[96] our numerical data on the transfer rate rate between adjacent A:T pairs refer to the situation where $k_f \ll k_{n\rightarrow(n+1)}$.

Table 3. Hole Transfer Rate between Adjacent A:T Pairs for Hairpin 6 with Different Values of the Localization Energy E_{loc}

		E_{loc} (meV)		
rate (ps^{-1})	no partial localization	50	150	250
$k_{1\rightarrow 2}$	0.65	0.36	0.23	0.18
$k_{2\rightarrow 3}$	0.98	0.41	0.24	0.20
$k_{3\rightarrow 4}$	1.53	1.08	0.90	0.49
$k_{4\rightarrow 5}$	21.23	3.96	1.35	0.78
$k_{5\rightarrow 6}$	86.16	4.31	2.31	1.83

The transfer rate, k_f, for the hole transition from the last base pair to the hole acceptor can be calculated by replacing k_{n+1} with the arrival rate, k_a, in eq 17. The values of k_f are listed in Table 4 for the hairpins **3**–**6**. The values of k_f for the hairpins **1** and **2** are not shown, since hole transfer along these two short hairpins is governed mainly by superexchange. Including partial localization in our model considerably reduces k_f. Similar to hole transfer rate between neighboring A:T base pairs, the increase of the localization energy reduces k_f by reducing the probability of thermal repopulation of the $|A_i\rangle$ states. The data in Table 4 show that the value of k_f depends not only on the value of E_{loc} but also on the length of the hairpin. This can be understood by taking into account that the increase of the hairpin length makes the energy gap between the last base pair and the hole acceptor larger, thus reducing the transfer rate between them. For example, k_f for hairpin **3** is equal to 0.93 ns^{-1} but becomes as small as 0.17 ns^{-1} for hairpin **6**. Note that the values of k_f are 3 orders of magnitude smaller than the typical hole transfer rates between adjacent base pairs (see Table 3). Hence, this last transfer step should be considered as the limiting factor for the overall hole migration process.

Table 4. Rates of Hole Transfer from the Last A:T Base Pair to the Acceptor (k_f) in Poly(A)-Poly(T) Hairpins with Different Values of the Localization Energy E_{loc}

	k_f (ns^{-1})			
		E_{loc} (meV)		
seq.	no partial localization	50	150	250
3	15.68	1.58	0.93	0.61
4	7.55	0.69	0.40	0.24
5	5.00	0.43	0.25	0.16
6	3.58	0.30	0.17	0.11

Charge-Transfer Mechanism. As discussed in Introduction section, mechanistic picture of the charge transfer in DNA often relies on the competition of coherent superexchange and incoherent multistep hopping. The former mechanism is assumed to be dominant for short sequences with a few base pairs, while the latter prevails for longer DNA molecules. As follows from Figure 2, our calculations also provide evidence in favor of superexchange hole transfer along short hairpins. To recognize this, it should be remembered that superexchange leads to an indirect charge transfer between S_a and S_b with only a small fraction of the charge density residing on the base pair bridging a hole donor and a hole acceptor. This, however, is not the case for long hairpins. Indeed, according to the data of Figure 3, in such systems the hole transfer cannot be associated with superexchange since most of the charge is located on the base pairs during the charge propagation. Now the hole transfer will proceed via another mechanism distinct from superexchange. This rises several important questions: (i) Can this alternative mechanism be incoherent hopping, so that the mechanistic picture of hole migration is based on the competition of coherent and incoherent processes? or (ii) can experimental and theoretical results obtained for short and long hairpins be explained in the framework of one unified mechanism of charge transfer?

If the answer to the question (i) is positive, then the mechanism competing with superexchange is often assumed to be incoherent multistep hopping. This mechanism occurs via incoherent sequential transitions of the charge carriers between adjacent base pairs. The nature of the hops and the degree of charge delocalization have long been a matter of contention between various groups. Recent electronic structure calculations have shown that the frontier molecular orbitals of adenine stacks are mainly localized on a single base.[99] The localization of the molecular orbitals is due to the strong energetic disorder along the stack compared to the couplings between adjacent base pairs.[99] Semiclassical calculations of the charge propagation have also shown that due to the fast trapping rate on A bases, the charge remains localized on a single base pair between successive hops.[64] Such sequential transitions between localized states associated with a separate nucleobases were not observed in our calculations. As seen in Figure 3, the hole density goes from a localized state on S_a to a

dx.doi.org/10.1021/ja3113998 | J. Am. Chem. Soc. XXXX, XXX, XXX–XXX

delocalized state along the base pair stack. Therefore our calculations suggest that transfer of positive charge cannot be associated with hopping mechanism involving sequential transitions between localized states provided by nucleobases.

A certain degree of hole delocalization has been suggested earlier to explain the propagation of a positive charge along extended DNA systems. Polaron-assisted models[58,59,61,62,65] and variable-range hopping approach[47,100] are two different methods that predict different degree of hole delocalization. In polaronic models the hole density is inhomogeneously distributed over few base pairs with a maximum of the hole density located at the center of the delocalization domain.[58,59,65] The charge propagation occurs then by reversible sequential hops between neighboring domains. Another mechanism is considered within the framework of the model of variable range hole hopping. According to refs 47 and 100, variable range hopping is based on charge propagation along localized and delocalized channels. Half of the charge density is injected in the delocalized channels and spreads instantaneously along the base pair stack, while the other half is injected in the localized channels and propagates sequentially between neighboring base pairs.[47,100]

The two models mentioned above, as most of the models proposed in the literature, ignore the presence of traps along the hairpin. According to semiclassical approach the presence of these traps should induce a localization of the charge carrier on a single base pair.[64] To the best of our knowledge, our approach is the first attempt to demonstrate that a full quantum description of trapping together with an accurate treatment of static and dynamic disorder along the hairpin leads to the complete delocalization of charge carriers over the entire system. However the charge density profile obtained with our approach is very different from the ones obtained with the variable range hopping or the polaronic models. As seen in Figure 3, the charge density is rapidly transferred from S_a to the first base pair. Due to the large energy difference between the first and the second A bases, a significant hole localization occurs on the first site. The charge density is then slowly transferred to the second base pair and so on. In contrast to the reversible hopping used by a number of authors, the transfer from base pair to base pair is here irreversible with charge density building up further and further away from S_a. Besides due to the dephasing induced by the dynamical disorder and the interactions between the propagating charge and the bath modes, the coherence of the propagating charge, i.e., the off-diagonal elements of its density matrix, progressively vanishes. This gradual loss of coherence transforms the initial pure state localized on S_a into a delocalized mixed state. This is in contrast with the polaron-based model where such decoherence can only be obtained by averaging the dynamics over the initial position and momentum of the sites. On the other hand, variable range hopping suggests an instantaneous loss of coherence and hence does not describe the transition between the initial pure state and the final mixed state.

The intermediate mechanism depicted in Figure 3 is due to the combined effects of the dynamic disorder and traps states. The dynamical disorder facilitates the transfer between neighboring base pairs by randomly creating resonance of their on-site energies. The degree of delocalization of the charge carrier is therefore gated by the dynamical disorder. A maximum degree of delocalization is obtained when the amplitudes of dynamic and static disorders are of the same order of magnitude. In addition, the characteristic time of fluctuations, τ, has to be small enough so that many accidental resonances can be created during the lifetime of the hole on the hairpin. On the other hand, τ must be large enough for the resonant transfer between bases to occur. These fluctuations as well as the interaction with the bath modes leads to a progressive loss of coherence for the propagation of hole density preventing superexchange to occur across 1−2 base pairs. As seen in Figure 4 the presence of traps along the system is crucial to obtain a quantitative agreement between theory and experiment. As one could expect the traps impede the charge transfer between neighboring bases and slow down the overall charge transfer. The presence of traps also affects the profile of the charge density. Ignoring the traps in hairpin **6** leads to smaller maximum population on the second base pair since the hole density does not undergo a strong localization on that site. As mentioned above, our model ignores the reorganization of the solvent induced by the hole motion.[57] The solvent reorganization can, in principle, localize the charge carriers.[63] However this solvent-induced localization requires that the propagation time and the time of solvent reorganization will be of the same order of magnitude. This mechanism is therefore important for long DNA molecules and can be neglected for the hairpins studied in the present paper. For the latter systems, our calculations predict that hole is transferred from the donor to the acceptor via one unified mechanism rather than through two competing mechanisms involving superexchange and hopping. This unified mechanism, which is truly intermediate between coherent superexchange and incoherent multistep hopping, is expected to occur on spatial scales intermediate between the length of DNA hairpins with 1−2 base pairs and the length of extended DNA oligomeric systems.

CONCLUSION

In this paper we formulated a model for hole transfer in relatively short poly(A)-poly(T) hairpins containing less that seven base pairs. We have analyzed the effect of partial localization of the hole density on the arrival rate on the acceptor site, the injection rate, and their corresponding quantum yields. Our calculations are based on the numerical solution of the Liouville equation with the Hamiltonian in which few molecular vibration modes are explicitly incorporated. This allows us to take into account the hole−phonon interactions responsible for partial localization of charge carriers.

Our calculations confirm that superexchange is indeed the mechanism governing the hole transfer from donor to acceptor in poly(A)-poly(T) hairpins with one or two base pairs. However, charge-transfer excitation of the stilbene-adenine sandwich pair may bypass the locally excited state, removing the need for the superexchange mechanism. For longer hairpins our simulations show a delocalization of the positive charge along the entire system. The impact of partial localization of the hole density on the arrival rate and its distance dependence have been studied numerically. Our calculations show that in the absence of partial localization, the value of the arrival rate obtained for relatively long hairpins is overestimated by 2 orders of magnitudes. The inclusion of partial localization in our model reduces significantly the value of the arrival rates making numerical results consistent with available experimental data. Furthermore, the agreement between theoretical and experimental results was found to be much better in comparison with earlier investigations.

dx.doi.org/10.1021/ja3113998 | J. Am. Chem. Soc. XXXX, XXX, XXX−XXX

The distance dependence of the arrival rate predicted by our model represents an exponential decay ($\propto e^{-\beta R}$ with $\beta = 0.9$ Å^{-1}) for short hairpins followed by a power law [$\propto (R/R_0)^{-\eta}$ with $\eta = 2$] as the hairpin becomes longer. These values of β and η were found to be in good agreement with experimental data and were previously associated with superexchange and multistep hopping, respectively. Our simulations provide evidence in favor of superexchange for short hairpins. However the power law distance dependence of the arrival rate alone cannot be considered as a signature of multistep incoherent hopping since a similar distance dependence was obtained in our simulations where the charge propagation is mediated by the delocalization of charge density along the entire sequence. The partial localization involved in the latter mechanism of charge propagation does not lead to a complete loss of coherence during hole motion. Consequently, the charge transfer along the short DNA hairpins considered in this article proceeds via an intermediate mechanism distinct of both superexchange and hopping. This intermediate mechanism should dominate if the characteristic time of hole transfer through the $|A_i\rangle$ states is larger than time needed for the localization of the positive charge due to the $|A_i\rangle \rightarrow |t_i\rangle$ transition but smaller than time required for the reorganization of the molecular surrounding. A similar mechanism could also occur during charge transfer in organic photovoltaics and photoelectric materials as the main ingredients responsible for charge propagation are the same as the ones described here. The presence of correlated molecular vibration modes in organic crystals could however change the degree of delocalization of the charge carrier.

The numerical results obtained following our approach also enable us to calculate the transfer rates between adjacent A:T pairs. Due to the site energy profile along the hairpin, this rate turns out to be larger at the end of the sequence than at the beginning. Besides, due to the large energy difference between the last base pair of the sequence and the hole acceptor, the transfer rate between these two sites is much smaller than all the transfer rates between adjacent A:T pairs. Consequently this last step should be consider as the limiting factor of the charge migration from the hole donor to the hole acceptor.

■ ASSOCIATED CONTENT

Supporting Information

Implementation and details concerning of the stochastic surrogate Hamiltonian; parametrization of the bath spectral density; parametrization of the dynamical disorder; evolution of the site population on hairpin **6**; and analysis of the trapping and detrapping rates. This material is available free of charge via the Internet at http://pubs.acs.org.

■ AUTHOR INFORMATION

Corresponding Author

n-renaud@northwestern.edu

Notes

The authors declare no competing financial interest.

■ ACKNOWLEDGMENTS

We would like to thank Ronnie Kosloff and Gil Katz for helpful discussions. This work was supported by the department of Navy, Office of Naval Research, under award N00014-11-1-0729.

■ REFERENCES

(1) Ratner, M. *Nature* **1999**, *397*, 480−481.
(2) Genereux, J.; Barton, J. *Chem. Rev.* **2010**, 1642−1662.
(3) *Charge Transfer in DNA: from theory to applications*;Wagenknecht, H.-A., Ed.; Wiley-VCH Verlag GmbH & Co. KGaA: Weinheim, Germany, 2006.
(4) *Long-Range charge transfer in DNA I and II*, Topics in Current Chemistry; Schuster, G. , Ed.; Springer-Verlag: Berlin, Germany, 2004; Vols. *236 and 237*.
(5) Kanvah, S.; Joseph, J.; Schuster, G. B.; Barnett, R. N.; Cleveland, C. L.; Landman, U. *Acc. Chem. Res.* **2010**, *43*, 280−287.
(6) Huang, Y.; Cheng, A. K. H.; Yu, H.-Z.; Sen, D. *Biochemistry* **2009**, *48*, 6794−6804.
(7) Guo, X.; Gorodetsky, A.; Hone, J.; Barton, J.; Nuckolls, C. *Nat. Nanotechnol.* **2008**, *3*, 163.
(8) Okamoto, A.; Tanaka, K.; Saito, I. *J. Am. Chem. Soc.* **2003**, *125*, 5066.
(9) Boon, E.; Ceres, D.; Drummond, T.; Hill, M.; Barton, J. *Nat. Biotechnol.* **2000**, *18*, 1096.
(10) Genereux, J.; Boal, A.; Barton, J. *J. Am. Chem. Soc.* **2010**, *132*, 891−905.
(11) Ito, T.; Rokita, E. *J. Am. Chem. Soc.* **2003**, *125*, 11480−11481.
(12) Breeger, S.; Hennecke, U.; Carell, T. *J. Am. Chem. Soc.* **2004**, *126*, 1302−1303.
(13) Tainaka, K.; Fujitsuka, M.; Takada, T.; Kawai, K.; Majima, T. *J. Phys. Chem. B* **2010**, *114*, 14657−14663.
(14) Park, M. J.; Fujitsuka, M.; Kawai, K.; Majima, T. *J. Am. Chem. Soc.* **2011**, *133*, 15320−15323.
(15) Daublain, P.; Thazhathveetil, A. K.; Shafirovich, V.; Wang, Q.; Trifonov, A.; Fiebig, T.; Lewis, F. D. *J. Phys. Chem. B* **2010**, *114*, 14265−14272.
(16) Lewis, F.; Liu, X.; Liu, J.; Miller, S.; Hayes, R.; Wasielewski, M. *Nature* **2000**, *406*, 51.
(17) Lewis, F.; Letsinger, R.; Wasielewski, M. *Acc. Chem. Res.* **2001**, *34*, 159−170.
(18) Kawai, K.; Kodera, H.; Osakada, Y.; Majima, T. *Nat. Chem.* **2009**, *1*, 156.
(19) Takada, T.; Kawai, K.; Fujitsuka, M.; Majima, T. *Proc. Natl. Acad. Sci. U.S.A.* **2004**, *101*, 14002−14006.
(20) Raytchev, M.; Pandurski, E.; Buchvarov, I.; Modrakowski, C.; Fiebig, T. *J. Phys. Chem. A* **2003**, *107*, 4592−4600.
(21) Meggers, E.; Michel-Beyerle, M. E.; Giese, B. *J. Am. Chem. Soc.* **1998**, 12950−12955.
(22) Berlin, Y. A.; Burin, A. L.; Ratner, M. A. *J. Am. Chem. Soc.* **2001**, *123*, 260−268.
(23) Senthilkumar, K.; Grozema, F. C.; Guerra, C. F.; Bickelhaupt, F. M.; Lewis, F. D.; Berlin, Y. A.; Ratner, M. A.; Siebbeles, L. D. A. *J. Am. Chem. Soc.* **2005**, *127*, 14894−14903.
(24) Grozema, F. C.; Tonzani, S.; Berlin, Y. A.; Schatz, G. C.; Siebbeles, L. D. A.; Ratner, M. A. *J. Am. Chem. Soc.* **2009**, *131*, 14204−14205.
(25) Berlin, Y. A.; Burin, A. L.; Ratner, M. A. *J. Phys. Chem. A* **2000**, *104*, 443−445.
(26) Giese, B. *Top. Curr. Chem.* **2004**, *130*, 151−164.
(27) Vura-Weiss, J.; Wasielewski, M.; Thazhathveetil, A.; Lewis, F. *J. Am. Chem. Soc.* **2009**, *131*, 9722−9727.
(28) Lewis, F.; Zhu, H.; Daublain, P.; Sigmund, K.; Fiebig, T.; Raytchev, M.; Wang, Q.; Shafirovich, V. *Photochem. Photobiol. Sci.* **2008**, *7*, 534−539.
(29) Kim, H.; Choi, O.; Sim, E. *J. Phys. Chem. C* **2010**, *114*, 20394−20400.
(30) Senthilkumar, K.; Grozema, F.; Guerra, C. F.; Bickelhaupt, F.; Siebbeles, L. *J. Am. Chem. Soc.* **2003**, *125*, 13658.
(31) Hush, N.; Cheung, S. *Chem. Phys. Lett.* **1975**, *34*, 11−14.
(32) Mishra, D.; Pal, S. *J. Mol. Struct. THEOCHEM* **2009**, *902*, 96−102.
(33) Voityuk, A. A.; Jortner, J.; Bixon, M.; Rosch, N. *Chem. Phys. Lett.* **2000**, *324*, 430−434.

(34) Lewis, F.; Zhu, H.; Daublain, P.; Fiebig, T.; Raytchev, M.; Wang, Q.; Shafirovich, V. *J. Am. Chem. Soc.* **2006**, *128*, 791−800.
(35) Lewis, F.; Zhu, H.; Daublain, P.; Cohen, B.; Wasielewski, M. *Ang. Chem. Ed. Int.* **2006**, *118*, 8150−8153.
(36) Lewis, F. D.; Daublain, P.; Cohen, B.; Vura-Weiss, J.; Wasielewski, M. *Ang. Chem., Ed. Int.* **2008**, *47*, 3798.
(37) Thazhathveetil, A.; Trifonov, A.; Wasielewski, M.; Lewis, F. *J. Am. Chem. Soc.* **2011**, *133*, 11485−11487.
(38) Kawai, K.; Hayashi, M.; Majima, T. *J. Am. Chem. Soc.* **2012**, *134*, 9406−9409.
(39) Jortner, J.; Bixon, M.; Langenbacher, T.; Michel-Beyrele, M. *Proc. Natl. Acad. Sci. U.S.A.* **1998**, *95*, 12759−12765.
(40) Grozema, F.; Berlin, Y.; Siebbeles, L. D. A. *J. Am. Chem. Soc.* **2000**, *122*, 10903−10909.
(41) Genereux, J.; Wuerth, S. M.; Barton, K. *J. Am. Chem. Soc.* **2011**, 386−3868.
(42) Grozema, F.; Tonzani, S.; Berlin, Y.; Schatz, G.; Sibbeles, L.; Ratner, M. *J. Am. Chem. Soc.* **2008**, *130*, 5157.
(43) Priyadarshy, S.; Risser, S. M.; Beratan, D. N. *J. Phys. Chem.* **1996**, *100*, 17678−17682.
(44) Murphy, C.; Arkin, M.; Jenkins, Y.; Ghatia, N. D.; Bossmann, S.; Turro, N.; Barton, J. *Science* **1993**, *262*, 1025−1029.
(45) Hall, D.; Holmin, R. E.; Barton, J. K. *Nature* **1996**, *382*, 731.
(46) Bixon, M.; Jortner, J. *J. Am. Chem. Soc.* **2001**, *123*, 12556−12567.
(47) Renger, T.; Marcus, R. *J. Phys. Chem. A* **2003**, *107*, 8404−8419.
(48) Bixon, M.; Giese, B.; Wessely, S.; Langenbacher, T.; Michel-Beyrele, M.; Jortner, J. *Proc. Natl. Acad. Sci. U.S.A.* **1999**, *96*, 11713−11716.
(49) Berlin, Y.; Ratner, M. A. *Radiat. Phys. Chem.* **2005**, *74*, 124−131.
(50) Giese, B.; Amaudrut, J.; Kholer, A.-K.; Spormann, M.; Wessely, S. *Nature* **2001**, *412*, 318.
(51) Kawai, K.; Takada, T.; Tojo, S.; Majima, T. *J. Am. Chem. Soc.* **2003**, *125*, 6842−6843.
(52) Giese, B.; Wessely, S.; Spormann, M.; Lindemann, U.; Meggers, E.; Michel-Beyerle, M. E. *Ang. Chem., Ed. Int.* **1999**, *38*, 996.
(53) Lewis, F. D.; Wu, T.; Liu, X.; Letsinger, R. L.; Greenfield, S. R.; Miller, S. E.; Wasielewski, M. *J. Am. Chem. Soc.* **2000**, 2889−2902.
(54) Lewis, F.; Letsinger, R. L.; Wasielewski, M. *Acc. Chem. Res.* **2001**, *34*, 159−170.
(55) Ratner, M. A. *Proc. Natl. Acad. Sci. U.S.A.* **2001**, *98*, 387−389.
(56) Segal, D.; Nitzan, A.; Davis, W. B.; Wasielewski, M.; Ratner, M. A. *J. Phys. Chem. B* **2000**, *104*, 3817.
(57) Basko, D. M.; Conwell, E. M. *Phys. Rev. Lett.* **2002**, *88*, 098102.
(58) Henderson, P. T.; Jones, D.; Hampikian, G.; Kan, Y.; Schuster, G. B. *Proc. Natl. Acad. Sci. U.S.A.* **1999**, *96*, 8353−8358.
(59) Conwell, E. M. *Proc. Natl. Acad. Sci. U.S.A.* **2005**, *102*, 8795−8799.
(60) Barnett, R. N.; Cleveland, C. L.; Joy, A.; Landman, U.; Schuster, G. B. *Science* **2001**, *294*, 567−571.
(61) Schuster, G. B. *Acc. Chem. Res.* **2000**, *33*, 253−260.
(62) Shao, F.; O'Neil, M. A.; Barton, J. K. *Proc. Natl. Acad. Sci. U.S.A.* **2004**, *101*, 17914−17919.
(63) Voityuk, A. A. *J. Chem. Phys.* **2005**, 204904.
(64) Olofsson, J.; Larsson, S. *J. Phys. Chem. B* **2001**, *105*, 10398−10406.
(65) Conwell, E. M.; Rakhmanova, S. V. *Proc. Natl. Acad. Sci. U.S.A.* **2000**, *97*, 4556−4560.
(66) Grozema, F.; Siebbeles, L.; Berlin, Y.; Ratner, M. *Chem. Phys. Chem.* **2002**, *03*, 536−539.
(67) Berlin, Y. A.; Burin, A. L. *Chem. Phys. Lett.* **1996**, *257*, 665−673.
(68) Siebbeles, L. D. A.; Berlin, Y. A. *Chem. Phys.* **1998**, *238*, 97−107.
(69) Berlin, Y.; Burin, A. L.; Ratner, M. A. *Chem. Phys.* **2002**, *275*, 61−74.
(70) Voityuk, A. A.; Siriwong, K.; Rosch, N. *Phys. Chem. Chem. Phys.* **2001**, *3*, 5421.
(71) Voityuk, A. A. *J. Chem. Phys.* **2008**, *128*, 115101.
(72) Voityuk, A. A. *J. Chem. Phys.* **2008**, *128*, 045104.
(73) O'Neil, M. A.; Becker, H.-C.; Wan, C.; Barton, J. K.; Zewail, A. H. *Ang. Chem. Ed. Int.* **2003**, *42*, 5896−5900.
(74) Bixon, M.; Jortner, J. *J. Phys. Chem. A* **2001**, *105*, 10322−10328.
(75) Breuer, H.; Petruccione, F. *The theory of open quantum system*; Oxford University Press: Oxford, U.K., 2002.
(76) Palimieri, B.; Abramavicius, D.; Mukamel, S. *J. Chem. Phys.* **2009**, *130*, 204512.
(77) Egorova, D.; Khul, A.; Domcke, W. *Chem. Phys.* **2001**, *268*, 105−120.
(78) Ishizaki, A.; Fleming, G. *J. Chem. Phys.* **2009**, *130*, 234111.
(79) Dalibard, J.; Castin, Y.; Molmer, K. *Phys. Rev. Lett.* **1992**, *68*, 580−583.
(80) Pillo, J.; Harkonen, K.; Maniscalco, S.; Suominen, K.-A. *Phys. Rev. A* **2009**, *79*, 062112.
(81) Katz, G.; Gelman, D.; Ratner, M. A.; Kosloff, R. *J. Chem. Phys.* **2008**, *129*, 034108.
(82) Katz, G.; Ratner, M. A.; Kosloff, R. *New J. Phys.* **2010**, *12*, 015003.
(83) Renaud, N.; Mujica, V.; Ratner, M. *J. Chem. Phys.* **2011**, 075102.
(84) Koch, C. P.; Kluner, T.; Freund, H. J.; Kosloff, R. *J. Chem. Phys.* **2002**, *106*, 7983−7996.
(85) Koch, C.; Kluner, T.; Kosloff, R. *Phys. Rev. Lett.* **2003**, *90*, 117601.
(86) Renaud, N.; Powell, D.; Zarea, M.; Movaghar, B.; Wasielewski, M. R.; Ratner, M. A. *J. Phys. Chem. A* article ASAP; DOI: 10.1021/jp308216y.
(87) Kumar, A.; Sevilla, M. D. *Chem. Rev.* **2010**, *110*, 7002−7023.
(88) Carra, C.; Iordanova, N.; Hammes-Schiffer, S. *J. Phys. Chem. B* **2002**, *106*, 8415−8421.
(89) Paavola, J.; Pillo, J.; Suominen, K.-A.; Maniscalco, S. *Phys. Rev. A* **2009**, *79*, 05120.
(90) Weiss, U. *Quantum Dissipative Systems*; World Scientific: Singapore, 1999.
(91) Wiorkiewicz-Kuczerat, J.; Karplus, M. *J. Am. Chem. Soc.* **1990**, *112*, 5324−5340.
(92) Taniguchi, M.; Kawai, T. *Phys. Rev. E* **2005**, *72*, 061909.
(93) Hess, S.; Gotz, M.; Davis, W. B.; Michel-Beyerle, M.-E. *J. Am. Chem. Soc.* **2001**, *123*, 10046−10055.
(94) Reid, G. D.; Whittaker, D. J.; Day, M. A.; Turton, D. A.; Kayser, V.; Kelly, J. M.; Beddard, G. S. *J. Am. Chem. Soc.* **2002**, *124*, 5518−5527.
(95) Lewis, F. D.; Liu, J.; Weigel, W.; Rettig, W.; Kurkinov, I. V.; Beratan, D. N. *Proc. Natl. Acad. Sci. U.S.A.* **2002**, *99*, 12536−12541.
(96) Takada, T.; Kawai, K.; Cai, X.; Sugimoto, A.; Fujitsuka, M.; Majima, T. *J. Am. Chem. Soc.* **2004**, *126*, 1125−1129.
(97) Wan, C.; Fiebig, T.; Kelley, S. O.; Treadway, C. R.; Barton, J. K.; Zewail, A. *Proc. Natl. Acad. Sci. U.S.A.* **1999**, *96*, 6014−6019.
(98) Conron, S. M. M.; Thazhathveetil, A. K.; Wasielewski, M. R.; Burin, A. L.; Lewis, F. D. *J. Am. Chem. Soc.* **2010**, *132*, 14388−14390.
(99) Kumar, A.; Sevilla, M. D. *J. Phys. Chem. B* **2011**, *115*, 4990−5000.
(100) Yu, Z. G.; Song, X. *Phys. Rev. Lett.* **2001**, *86*, 6018−6021.